HHS Public Access

Author manuscript

ACS Appl Mater Interfaces. Author manuscript; available in PMC 2021 April 30.

Published in final edited form as:

ACS Appl Mater Interfaces. 2019 August 14; 11(32): 28641–28647. doi:10.1021/acsami.9b07648.

Significant Suppression of *S. aureus* Colonization on Intramedullary Ti6Al4V Implants Surface-grafted with Vancomycin-bearing Polymer Brushes

Ben Zhang, **Benjamin M. Braun**, **Jordan D. Skelly**, **David C. Ayers**, **Jie Song***

Department of Orthopedics & Physical Rehabilitation, University of Massachusetts Medical School, Worcester, MA 01655, USA

Abstract

Orthopedic implant associated bacterial infection presents a major health threat due to tendency for periprosthetic bacteria colonization/biofilm formation which protects bacteria from host immune response and conventional antibiotic treatment. Using surface-initiated atom transfer radical polymerization (SI-ATRP) and copper-catalyzed azide-alkyne cycloaddition (CuAAC), alkynylated vancomycin is conjugated to azido-functionalized side chains of polymethacrylates grafted from Ti6Al4V. High-efficiency CuAAC across the substrate is confirmed by complete surface conversion of azides by X-ray photoelectron spectroscopy (XPS) and elemental mapping of changing characteristic elements. The vancomycin-modified surface (Ti-pVAN) significantly reduces *in vitro* adhesion and colonization of *Staphylococcus aureus (S. aureus),* a main bacterial pathogen responsible for periprosthetic infection and osteomyelitis, compared to untreated Ti6Al4V, supporting retained antibacterial properties of the covalently conjugated antibiotics. When the surface-modified intramedullary Ti-pVAN pins are inserted into mouse femoral canals infected by bioluminescent Xen-29 *S. aureus*, significantly reduced local bioluminescence along with mitigated blood markers for infection are detected compared to untreated Ti6Al4V pins over 21 days. Ti-pVAN pins retrieved after 21 days are confirmed with ~20-fold reduction in adherent bacteria counts compared to untreated control, supporting the ability of surface-conjugated vancomycin in inhibiting periprosthetic *S. aureus* adhesion and colonization.

Table of Contents (TOC)/Abstract Graphic

*Corresponding Author jie.song@umassmed.edu (J.S.).

ASSOCIATED CONTENT

Supporting Information. Synthetic scheme of AzTEGMA and VAN-PEG7-ALK; high-resolution XPS scans for Cl2p and N1s of the Ti-pVAN pin; *in vivo* study design; key/scavenger organ pathology; representative histology of the explanted femur.

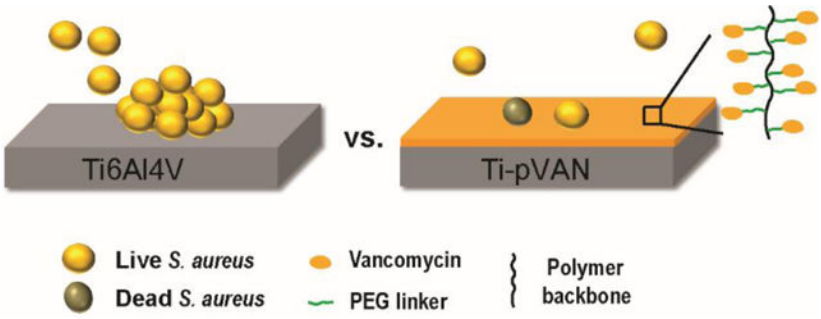

Keywords

periprosthetic infection; surface-initiated atom transfer radical polymerization; copper-catalyzed azide-alkyne cycloaddition; vancomycin; *Staphylococcus aureus*

1. INTRODUCTION

Periprosthetic infection is one of the most serious complications in orthopedic surgeries, occurring in 1–4% of primary arthroplasties and up to 30% of revision arthroplasties,[1,2] and exhibits an alarming upward trend despite rigorous prophylaxis and surgical approaches.[3,4] Patients suffering from these infections are often subjected to prolonged antibiotic therapy, multiple follow-up surgeries or even amputation, resulting in tremendous agony (5-fold increase in mortality) and economic burden.[5–7] *S. aureus*, a gram positive bacterium and the main cause of osteomyelitis, accounts for 34% of all orthopedic implant related infections.[8,9] Foreign implant surfaces tend to encourage the colonization and biofilm formation of pathogens such as *S. aureus* (e.g. the inoculated dose of bacteria required to establish a joint infection is 100-fold lower for prosthetic joints than native joints[10]), with the dense biopolymer matrices protecting the bacteria from host immune response and conventional antibiotic treatments.[11] Thus, implant surface modifications that effectively inhibit *S. aureus* adhesion/colonization and biofilm formation are of significant clinical interest. Towards this goal, reducing bacterial adhesion (e.g. via surface topology engineering,[12] antifouling polymer coating[13]) and introducing bactericidal properties are two commonly pursued strategies. The latter strategy more directly aligns with the ultimate clinical goal, but current technologies are inadequate. For instance, delivering physically encapsulated antibiotics (e.g. via hydrogels[14] or meshes[15]) to implant surface[16,17] often results in sub-optimal drug release kinetics or cytotoxicity associated with the excessive antibiotics delivered.[18,19] On the other hand, covalent tethering a monolayer of antibiotics via esterification/amidation chemistry to surface oxides of metal alloy implants[20,21] was limited by the achievable drug density and relatively short-term efficacy (e.g. 2-week inhibition in rodents[22]). We hypothesize that antibiotics covalently conjugated to polymer brushes grafted from metallic implant surface where the drug density can be prospectively altered could bridge the gap of existing methods to inhibit bacterial growth and colonization.

To test the hypothesis, we chose to covalently attach alkynylated vancomycin through efficient copper-catalyzed azide-alkyne cycloaddition (CuAAC) “click” chemistry to azide-bearing polymethacrylates surface-grafted from Ti6Al4V alloy, a common orthopedic

metallic hardware,[23–26] via SI-ATRP (Figure 1). Vancomycin, a glycopeptide antibiotic acting at the Gram-positive bacterial cell walls to block peptidoglycan synthesis, is considered the most effective in treating infections caused by *Staphylococcus* including Methicillin-resistant *S. aureus*.[1,27] It is known to inhibit the transpeptidation and transglycosylation steps of bacterial cell wall biosynthesis through the binding of the L-Lys-D-Ala-D-Ala termini of the nascent peptidoglycan precursor through 5 sets of H-bonds.[28–30] Of the 3 potential functionalization sites (carboxyl, N-methylleucyl or N-vancosaminyl), the N-vancosaminyl site farthest away from the critical binding region was chosen for installing the alkynyl reactive handle, through a flexible hydrophilic oligo(ethylene glycol) linker (PEG7, Scheme S1), to maintain antibiotic activity of covalently tethered vancomycin. We chose to graft polymethacrylates with azide-bearing sidechains from Ti6Al4V using SI-ATRP to ensure good surface coverage by the polymers before conjugating alkynylated vancomycin to their side chains via "click" reaction. This strategy is preferred over directly grafting polymerizable vancomycin derivatives[30–32] due to concerns over the steric hindrance that bulky monomers might impose on the SI-ATRP.

2. EXPERIMENTAL SECTION

2.1. Materials.

All chemicals were purchased from Sigma-Aldrich, TCI or BroadPharm, and used as received unless noted otherwise. Triethylamine was dried by calcium hydride and distilled before use. Ti6Al4V plates (0.5-mm thick, TMS Titanium, Poway, CA) were cut into 1×1 cm^2 square pieces and Ti6Al4V wires (0.5 mm in diameter, Goodfellow Corporation, Coraopolis, PA) were cut into 1-cm long pins, polished under water with 600, 1500, and 3000 grit silicon carbide sandpapers, and bath-sonicated sequentially in DI water (10 min), acetone (10 min), dichloromethane (10 min), hexane (10 min), dichloromethane (10 min), and acetone (10 min), followed by annealing at 120 ºC in a vacuum oven for 12 h and 2-min air plasma cleaning (Harrick, PDC-001). *Staphylococcus aureus* (*S. aureus*) (ATCC 25923) and bioluminescent *S. aureus* strain Xen29 were purchased from ATCC and PerkinElmer, respectively. Both strains are susceptible to vancomycin treatment.

2.2. General Instrumentation.

^{1}H NMR (500 MHz) and ^{13}C NMR (125 MHz) were recorded on a Bruker spectrometer. Chemical shifts of ^{1}H and ^{13}C NMR were calibrated using the residual solvent peak. Mass spectra were acquired on a Thermo LTQ in a positive ion mode. The optical density of bacterial culture was measured at 600 nm on a Cary 50 UV-Vis Spectrophotometer. Bioluminescence imaging was carried out on an *in vivo* imaging system (IVIS) (PerkinElmer IVIS-100).

Gel permeation chromatography (GPC).—GPC was carried out on a Varian Prostar HPLC system equipped with two Agilent 5-mm PLGel MiniMIX-D columns, a UV–vis detector and a 1260 Infinity evaporative light scattering detector (Agilent Technologies). Tetrahydrofuran (THF) was used as an eluent at a flow rate of 0.3 mL/min at RT. M_n and PDI were calculated by the Cirrus AIA GPC Software using the narrowly dispersed

polystyrenes (ReadyCal kits, PSS Polymer Standards Service, Germany) as calibration standards.

X-ray photoelectron spectroscopy (XPS).—Surface compositional analyses of functionalized Ti6Al4V substrates were carried out on a Thermo Scientific K-Alpha XPS equipped with an Al K_α radiation source under the pass energy of 200 or 50 eV (for survey or high-resolution scan) and the spot size of 400 μm. Survey scan spectra were obtained from five consecutive scans of a randomly chosen area of interest while high resolution scan spectra were obtained from ten consecutive scans. All binding energies were referenced to the C1s hydrocarbon peak at 285.0 eV.

Water contact angle measurements.—Static water contact angles on flat functionalized Ti6Al4V substrates were recorded on a CAM200 goniometer (KSV Instruments). About 50-L droplet of Milli-Q water was placed on the substrate and the contact angles of the droplet were recorded after 30 s. The reported contact angles were averaged from three randomly selected regions on each substrate and the left and right contact angles of each droplet.

2.3. Synthesis of Functional Monomer and Alkynylated Vancomycin and Functionalization of Ti6Al4V by SI-ATRP.

The syntheses of the functional monomer AzTEGMA and alkynylated vancomycin VAN-PEG7-ALK were carried out as shown in Scheme S1. Ti-Br was prepared and characterized per our prior reported procedure.[33]

AzTEG.—To a solution of NaN_3 (10 g, 0.15 mol) in 60 mL of DI water, 2-(2-(2-chloroethyoxy)ethoxy)-ethanol (17 g, 0.10 mol) was added. The reaction mixture was heated to 70 ºC and kept overnight. After cooling down to room temperature (RT), the aqueous solution was extracted with diethyl ether (3×50 mL) and dried with $MgSO_4$ before solvent removal under vacuum to yield 14 g of colorless oil (80 %). ^{1}H NMR (500 MHz, $CDCl_3$, δ/ppm): 3.74 (m, 2H), 3.68 (m, 6H), 3.62 (m, 2H), 3.40 (m, 2H); ^{13}C NMR (125 MHz, $CDCl_3$, δ/ppm): 72.51, 70.68, 70.39, 70.06, 61.79, 50.68. ESI-MS, positive mode (m/z): 198.5 $[M+Na]^+$ (cal.:198.1 for $[M+Na]^+$).

AzTEGMA.—Methacryloyl chloride (0.60 g, 5.7 mmol) in 10 mL of CH_2Cl_2 was added dropwise into 10-mL CH_2Cl_2 solution of AzTEG (1.0 g, 5.7 mol) and trimethylamine (TEA) (0.57 g, 5.7 mmol) at 0 ºC under argon atmosphere. The reaction was gradually warmed up to RT and kept overnight. After filtration, the solvent was removed under vacuum and the residue was subjected to silica-gel column chromatography (Ethyl acetate/hexane=1/5, v/v) to obtain 0.8 g colorless product (58%). ^{1}H NMR (500 MHz, $CDCl_3$, δ/ppm): 6.13 (s, 1H), 5.57 (s, 1H), 4.31 (m, 2H), 3.75 (m, 2H), 3.67 (m, 6H), 3.38 (m, 2H), 1.95 (m, 3H); ^{13}C NMR (125 MHz, $CDCl_3$, δ/ppm): 167.72, 136.51, 126.08, 71.06, 70.45, 69.59, 64.19, 51.04, 18.65. ESI-MS, positive mode (m/z): 198.5 $[M + Na]^+$ (cal.:266.1 for $[M+H]^+$).

VAN-PEG7-ALK.—Vancomycin hydrochloride (100 mg, 0.067 mmol) and NHS-PEG7-ALK (33 mg, 0.067 mmol) were dissolved in 1 mL of dimethylformamide (DMF) and then

trimethylamine (30 mg, 0.30 mmol) was added dropwise at RT. The solution was stirred for 24 h and then precipitated into 15 mL of diethyl ether at 0 °C. After centrifugation at 8000 rpm for 5 min, the pelleted solid was dissolved in 2 mL of mixture of acetonitrile and water (1/1, v/v) and desalted in a dialysis membrane tubing (Spectra/Por 6, MWCO: 1000) against acetonitrile and water (1/1, v/v) for 24 h, with regular change of fresh solvent every 6 h. The desalted solution was lyophilized to obtain 45 mg of white product (37%). ^{1}H NMR (500 MHz, d_6-DMF, δ/ppm): 6.13 (s, 1H), 5.57 (s, 1H), 4.31 (m, 2H), 3.75 (m, 2H), 3.67 (m, 6H), 3.38 (m, 2H), 1.95 (m, 3H); ^{13}C NMR (125 MHz, $CDCl_3$, δ/ppm): 173.88, 170.77, 170.26, 169.56, 168.52, 167.63, 158.7, 158.44, 158.06, 157.64, 156.44, 153.67, 152.61, 150.98, 149.72, 143.34, 141.95, 141.87, 141.68, 138.59, 136.80, 133.05, 128.53, 128.52, 128.24, 127.81, 127.32, 126.62, 125.28, 125.16, 124.24, 124.19, 122.61, 118.62, 117.34, 108.40, 105.54, 103.08, 102.42, 98.8, 80.95, 79.08, 78.73, 77.49, 76.69, 73.30, 72.61, 71.42, 70.76, 70.65, 70.14, 69.59, 68.00, 64.17, 63.71, 63.48, 62.47, 61.26, 59.58, 58.35, 56.23, 55.18, 55.04, 54.94, 51.81, 38.07, 25.21, 23.82, 23.40, 22.38, 17.88. ESI-MS, positive mode (m/z): 922.8 $[M+Na+H]^{2+}$ (cal.:922.8 for $[M+Na+H]^{2+}$). The minimal inhibitory concentration of VAN-PEG7-ALK against *S. aureus* was determined as 10 μg/ml (Figure S1).

Ti-pAz.—2,2’-bipyridyl (14 mg, 0.09 mmol) and trifluoroethanol (1 mL) were charged into a dry Schlenk flask. After three “freeze-pump-thaw” cycles to remove oxygen, the flask was back filled with argon followed by the addition of CuBr (5.2 mg, 0.033 mmol) under argon protection. The mixture was stirred for 5 min until a uniform dark brown catalyst complex was formed. AzTEGMA (440 mg, 1.8 mmol) and TFE (1 mL) were charged into another dry Schlenk flask containing Ti-Br substrates, and degassed by three “freeze-pump-thaw” cycles. SI-ATRP was initiated upon catalyst complex injection via a syringe and proceeded for 12 h at RT. Polymer formed in solution was passed through a pad of silica gel (Alfa Aesar, silica gel 60, mesh 230–400) to remove copper catalyst before it was dried under vacuum and subjected to GPC characterization, which revealed a number average molecular weight (M_n) of 86 kDa and a polydispersity index (PDI) of 1.4. Meanwhile, Ti-pAz substrates were washed with 50 mL of acetone (30-min stirring, repeated three times) to remove the free polymers physically absorbed on the surface before being dried under vacuum.

Ti-pVAN.—2,2’-bipyridyl (14 mg, 0.09 mmol) was dissolved in 0.5 mL of DMF and degassed via three “freeze-pump-thaw” cycles in a Schlenk flask, followed by the addition of CuBr (5.2 mg, 0.033 mmol) under argon protection. VAN-PEG7-ALK (20 mg, 0.01 mmol) dissolved in 1 mL of anhydrous DMF was charged in another dry Schlenk flask containing Ti-pAz substrates and degassed by three “freeze-pump-thaw” cycles, followed by the injection of half of the freshly prepared ATRP catalyst complex. The reaction proceeded at RT for 12 h with vortexing and then the Ti-pAz substrates were retrieved and washed with 70 mL of acetone (30-min stirring, repeated three times) to remove the free polymers physically absorbed on the surface before being dried under vacuum.

2.4. *In Vitro* Anti-bacterial Properties.

***In vitro* bacterial culture on Ti6Al4V plates.—**Sterilized Ti6Al4V and Ti-pVAN plates were each immersed in 1-mL *S. aureus* in Luria broth (LB) (1.2×10^5 CFU/mL) in a 24-well plate, and incubated for 5 h at 37 ºC with a shaking speed of 1 Hz. The retrieved plates were gently rinsed with 1-mL PBS three times and the adherent bacteria was fixed by 2% glutaraldehyde and air dried for scanning electron microscopy. For imaging by bioluminescence, 1-mL of bioluminescent Xen-29 in LB (2.3×10^6 CFU/mL) was added to each Ti6Al4V or Ti-pVAN plate in a 24-well plate and cultured for 7 h at 37 ºC at a shaking speed of 1 Hz. The retrieved plates were washed with 1-mL LB three times before being subjected to imaging on an IVIS-100 (n = 3; exposure time: 30 s).

Scanning electron microscopy (SEM).—The Ti6Al4V and Ti-pVAN plates retrieved from *S. aureus* culture were fixed with 2% EM-grade glutaraldehyde, serial-dehydrated/critical-dried, coated with Au (8 nm in thickness) and imaged on a Quanta 200 FEG MKII scanning electron microscope (FEI Inc., Hillsboro, OR) under high vacuum at an accelerating voltage of 8 kV.

2.5. *In vivo* studies.

The animal study was carried out per procedures approved by the University of Massachusetts Medical School Institutional Animal Care and Use Committee (IACUC). Skeletally mature CL57BL/6 mice (male and female; 8–12 weeks old) were used. To enable longitudinal monitoring of the infection in the mouse femoral canal treated with unmodified Ti6Al4V intramedullary (IM) pin or Ti-pVAN pin, bioluminescent Xen-29 *S. aureus* was diluted into 10^4 CFU/mL stock solution in LB for surgical injection. The *in vivo* study design, longitudinal follow-up by IVIS and micro computed tomography (μ-CT), as well as end-point femoral histology and bacterial count on retrieved pin are described in Figure S2.

Animal surgery.—The CL57BL/6 mice were anesthetized with 2–5% isoflurane in oxygen by inhalation and sterile-prepared for surgery. The mouse was placed in the supine position and an incision was made over the knee. With the joint exposed, a medial parapatellar arthrotomy was created and the patella and patellar tendon were put laterally to visualize the intercondylar notch of the femur. A 25-gauge hypodermic needle was used to broach and ream the femur. A gas-tight 10-μL syringe (Hamilton, Reno, NV, USA) was used to draw up 4 μL of either sterile LB solution or Xen-29 *S. aureus* solution (10^4 CFU/mL) for injection into the reamed femoral canal. Care was taken to ensure there was no overflow outside of the femur. A sterile unmodified Ti6Al4V or Ti-pVAN pin (~10 mm long and 0.5 mm in diameter) was then inserted into the femoral canal. The patella was returned to an anatomic position, and the skin was closed with 4–0 nylon suture. The animals were observed while recovering from anesthesia until they were able to fully support their own weight. Post-operative analgesia was accomplished with subcutaneous injections of buprenorphine every 12 hours for the first 48 hours following surgery.

***In vivo* bioluminescent imaging.—**Animals were imaged on post-operative days 7, 14, and 21 with an IVIS-100 imaging instrument. Mice were induced with isoflurane-oxygen anesthesia (2%) and placed supine in the imaging cabinet. The images were acquired over 5

min exposure and the bioluminescence intensity was quantified by placing a 20 pixel by 20 pixel region of interest over each femur. Background luminescence was subtracted using mouse implanted with Ti pin injected with 4-μL LB medium without bacteria

***μ*-CT.—**Mice were scanned the day after operation (day 1) and at 21 days post operation on a Scanco vivaCT 75 system (Scanco Medical, Switzerland) at an effective voxel size of 20.5×20.5×20.5 μm^3. The proximal and distal femoral growth plates were used to determine the center slice of the femur and 100 consecutive slices were analyzed on both sides for a total analysis length of ~4 mm. For all quantifications, the bone marrow space was excluded. A global threshold of 260 (minimum bone densities of 549.7 mg HA/cm^3 and above) was applied to calculate bone volume fraction (BVF) using Scanco Medical's analysis software. When analyzing cortical thickness, a threshold of 50 (minimum bone densities of 63.2 mg HA/cm^3 and above) was utilized to include the entire contoured cortical bone space despite some porosity within the cortical bone/around the endosteal surface.

Complete blood counts.—Blood was collected from mouse facial vein 7 days before, 7 days after, and 21 days after surgery. Complete blood count (CBC) was carried on an Abaxis VetScan HM5 instrument.

Quantification of Xen29 *S. aureus* bound to the retrieved IM pins.—At the 21-day or 4-month endpoint, the mice were sacrificed following the μ-CT scan. The metal pins were retrieved from the explanted femur of sacrificed mice and immediately put in 1-mL cold LB (4 ºC) and vortex for 5 min. A portion of each vortexed solution (20 μL) was loaded to a P100 agar plate and dispersed uniformly with a spreader. The agar plates were incubated at 37 ºC for 12 h to determine the bacterial CFU counts.

Femoral histology and key/scavenger organ pathology.—After the IM pin removal, the femoral explants retrieved at day 21 were immediately fixed in periodate-lysine-paraformaldehyde (PLP) fixative for 48 h at 4 ºC followed by decalcification in 18% aqueous ethylenediaminetetraacetic acid (EDTA, pH 8.0) for 2 weeks with bi-weekly changes of EDTA solution.[34] The decalcified explants underwent serial dehydration, paraffin embedding, and longitudinal sectioning (6 μm sections) before being stained for hematoxylin and eosin (H&E) for cellularity and by a gram stain kit (Abcam) for gram positive *S. aureus* (blue).

Heart, lung, kidney, liver, pancreas, spleen, and ribs were retrieved at 4 months post operation in a subset of animals and fixed and stained by H&E for comparison with organs retrieved from healthy age-matched controls. All histology images were taken at 50× and 200× magnifications.

2.6. Statistics.

All statistical analysis was performed using Prism 7.0 (GraphPad Software Inc., La Jolla, CA). Shapiro-Wilk normality testing was used to evaluate data distribution. Pair-wise comparisons passing normality test were analyzed with Student's t-test. Multiple group comparisons passing normality test were analyzed using one-way analysis of variance (ANOVA) with Tukey's posthoc while non-parametric multiple group comparisons were

analyzed using the Kruskal-Wallis test. Multi-variant comparisons were carried out using two-way ANOVA with Tukey's posthoc test. P-values of <0.05 were considered significant. All data was presented as mean ± standard error of the mean (S.E.M.).

3. RESULTS AND DISCUSSION

3.1. Ti6Al4V Substrates were Surface-modified with Vancomycin-bearing Polymer Brushes by SI-ATRP and CuACC

As shown in Figure 1, α-bromoisobutyryl initiator was first immobilized to the surface of Ti6Al4V via a phosphonic acid linker as previously described,[33] with the binding energies for the bromium (broad peak ~70 eV corresponding to Br3d) and phosphorus (sharp peak ~134 eV corresponding to P2p) that were absent from Ti6Al4V but characteristic for Ti-Br detected by XPS (Figure. 2a, red vs. black traces). SI-ATRP of functional monomer AzTEGMA, prepared from tri(ethylene glycol) chloride in two steps (Scheme S1), was then carried out on Ti-Br substrates. GPC characterization of the poly[2-(2-(2-azidoethyoxy)ethoxy)ethyl methacrylate] (pAzTEGMA) formed in solution revealed a number average molecular weight (M_n) of 86 kDa and a polydispersity index (PDI) of 1.4, which was previously shown to approximate those cleaved off the surface following the SI-ATRP.[33,35] Successful grafting of the azido-functionalized polymer brushes on Ti-pAz resulted in the disappearance of XPS signals associated with the surface initiator (Br3d & P2p) and the appearance of the N1s signals characteristic for azide (401 and 404 eV corresponding to terminal N's and the center N^+ of azide, respectively; Figure 2a, blue vs. red traces), consistent with our prior report.[33] The resulting Ti-pAz substrates were then further functionalized with alkynylated vancomycin VAN-PEG7-ALK (structure shown in Scheme S1), prepared from vancomycin and N-hydroxysuccinimide (NHS) ester of mono-alkynylated PEG7, by CuAAC to obtain the drug-conjugated Ti-pVAN substrates. The flexible PEG7 linker effectively reduced the steric hindrance of vancomycin, resulting in the full surface conversion of side chain azides on Ti-pAz to the triazoles upon CuACC as supported by the disappearance of the XPS signal at 404 eV (N^+) and appearance of the chlorine signal (~201 eV for Cl2p) only present in vancomycin for Ti-pVAN (Figure. 2a, green vs. blue traces). Furthermore, XPS elemental mapping of N1s and Cl2p over 400 μm×400 μm areas further confirmed the uniform enhancement of these characteristic surface element signals on Ti-pVAN vs. unmodified Ti6Al4V (Figure 2b). Finally, increases in water contact angles were observed upon surface modifications (Figure 2c), reflecting an increased surface hydrophobicity after vancomycin conjugation. Overall, these data support successful high-density surface grafting of vancomycin-bearing polymers with excellent surface coverage, which would be crucial to confer its ability to inhibit bacterial colonization across the functionalized substrate. It is worth noting that surface grafted vancomycin-bearing polymers remained stable after 2-week incubation in PBS (pH 7.4) as shown by readily detected Cl2p signal (Figure S3).

3.2. Ti6Al4V Substrates Surface-modified with Vancomycin-bearing Polymer Brushes Suppressed *S. aureus* Colonization and Growth *in Vitro*.

The ability of the vancomycin modified plates (Ti-pVAN) to inhibit the colonization and growth of *S. aureus* was first examined *in vitro*. After incubating Ti-pVAN or unmodified

plates in the *S. aureus* suspension (1.2×10^5 CFU/mL) in Luria broth (LB) medium at 37 ºC on a shaking incubator for 5 h, the plates were rinsed with phosphate buffered saline (PBS) and DI water before subjected to imaging by scanning electron microscopy (SEM). Whereas significant colonization of *S. aureus* (3D aggregates) was consistently detected across the untreated plate by 5 h (Figure 3a, top), *S. aureus* was only sparsely detected as lightly connected cellular patches on Ti-pVAN (Figure 3a, bottom). In parallel, Xen29 *S. aureus*, which emits bioluminescence when metabolically active due to the expression of luciferase, [36] was also cultured on these plates. Ti-pVAN plates yielded weaker luminescent signal than those cultured on the untreated plates (Figure 3b), further supporting the antibacterial property of the vancomycin covalently coupled to the surface grafted polymer brushes. Biofilm development of *S. aureus* on substrates usually involves several stages,[37,38] including initial adhesion, confluent cell sheet formation, micro/macrocolony development, and biofilm dispersal. Here we show that the antibacterial property of Ti-pVAN translated into early inhibition of the colonization and growth of *S. aureus* which are crucial to inhibiting mature biofilm formation.

3.3. Ti6Al4V Pins Surface-modified with Vancomycin-bearing Polymer Brushes Suppressed *S. aureus* Colonization and Reduced Infection in the Mouse Intramedullary Canal.

To examine the *in vivo* efficacy of this surface modification strategy, Ti6Al4V pins (0.5 mm in diameter) emulating the metallic component of total joint replacement hardware inserted into the intramedullary (IM) space of long bone were modified and characterized by XPS in the same fashion (Figure S4). A mouse femoral canal infection model involving inoculating a low dose of 40 CFU bioluminescent Xen29 *S. aureus* in reamed femoral canal followed by the insertion of an unmodified Ti6Al4V or a modified Ti-pVAN IM pin was utilized to emulate a realistic clinical scenario where gross contamination during arthroplasty surgery is rare. The degree of infection was longitudinally monitored by bioluminescence in the femoral canal, bacterial counts on retrieved pins, complete blood counts, as well as femoral thickening by μ-CT, femoral histology and key/scavenger organ pathology at the 21-day endpoint. Proper pin position was validated with post operation μ-CT (Figure 4a). Overall, bioluminescence intensity increased over time in the Xen29 infected group inserted with unmodified IM pins while decreased in the group treated with Ti-pVAN pins, culminating in significantly lower (~30%) bioluminescent signals in the latter by 21 days (Figure 4b). This result was accompanied with more drastic reduction (~20-fold) in the amount of *S. aureus* recovered from the retrieved Ti-pVAN pin (68 CFU) vs. that on the unmodified pins (~1500 CFU) on day 21 (Figure 4c), supporting significant *in vivo* inhibition of bacterial adhesion/colonization on the Ti-pVAN implant surface. Increasing monocytes and neutrophils were detected from the peripheral blood collected (complete blood counts/CBC) from the infected mice receiving unmodified pins over 21 days (Figure 4d), consistent with an innate immune response to the bacterial infection. By contrast, the Ti-pVAN treated group did not show significant changes in CBC, consistent with a mitigated local infection and a lack of sever systemic immune responses. In a small set of mice, an infected group treated with Ti-pVAN pins and kept for longer-term observation showed that key/scavenger organs remained normal at 4 months post-surgery (Figure S5, n=3) and that the bacterial counts from

retrieved pins remained low, with 3 out of the 4 pins evaluated showing 0 CFU while the other showing 50 CFU (n = 4).

Interestingly, some of the femurs in the *S. aureus* infected groups showed cortical thickening and bone loss (decreased bone volume fraction) by 21 days that are consistent with osteomyelitis complications,[39,40] although the changes were not statistically significant as revealed by μ-CT quantifications (Figure 5a). Femoral histology (H&E) confirmed cortical thickening in some of the infected mouse femurs in both pin treatment groups (Figure S6) and the presence of *S. aureus* along the thickened endosteal bone surface shown by gram staining (Figure 5b). These observations suggest that the vancomycin tethered on surface-grafted polymers were only able to exert “short-range” protection against bacterial colonization/growth on the implant surface. Without free vancomycin that could diffuse towards the endosteal bone surface, bacteria further away from the implant were not completely eradicated, consistent with the small amount of luminescence signals still detected in the Ti-pVAN treated group by 21 days (Figure 4b). Nevertheless, the overall reduction in bacteria colonized on the Ti-pVAN implant surface is clinically meaningful as planktonic *S. aureus* remained in the marrow cavity are likely more susceptible to host immune response or conventional systemic antibiotic treatment applied following surgery.[6]

4. CONCLUSIONS

In summary, we have developed a new surface modification strategy to covalently conjugate vancomycin through a flexible linker to the side chains of polymethacrylates surface-grafted from Ti6Al4V implants. The combination of SI-ATRP and highly efficient CuAAC “click” conjugation ensured excellent surface coverage by the polymers and high density presentation of vancomycin. The covalently tethered vancomycin effectively suppressed *S. aureus* colonization on the metallic substrates. Mouse studies further confirmed that vancomycin modified titanium pins inserted in femoral canals infected with *S. aureus* also significantly suppressed the bacterial colonization on the implant surface compared with those treated with unmodified pins, resulting in mitigated infections / immune responses. This surface modification strategy may be extended to covalently present other antibacterial functional groups to combat periprosthetic infections. The synergy of this surface modification strategy and conventional pre/post-operative systemic administration of antibiotics or other therapeutics[41] in eradicating periprosthetic infections remains to be determined.

Supplementary Material

Refer to Web version on PubMed Central for supplementary material.

ACKNOWLEDGEMENTS

The authors thank April Mason-Savas for histology support. This work was supported by NIH grant R01AR068418. XPS was performed at the Center for Nanoscale Systems (CNS) at Harvard University supported by the National Science Foundation award 1541959.

REFERENCES

(1). Donlan RM, Biofilm Formation: A Clinically Relevant Microbiological Process. Clin. Infect. Dis. 2001, 33 (8), 1387–1392. [PubMed: 11565080]

(2). Lynch AS; Robertson GT, Bacterial and Fungal Biofilm Infections. Annu. Rev. Med. 2008, 59, 415–428. [PubMed: 17937586]

(3). Kurtz SM; Lau E; Schmier J; Ong KL; Zhao K; Parvizi J, Infection Burden for Hip and Knee Arthroplasty in the United States. J. Arthroplasty 2008, 23 (7), 984–991. [PubMed: 18534466]

(4). Auerbach A, Healthcare Quality Measurement in Orthopaedic Surgery: Current State of the Art. Clin. Orthop. Relat. Res. 2009, 467 (10), 2542–2547. [PubMed: 19381743]

(5). Kurtz SM; Lau E; Watson H; Schmier JK; Parvizi J, Economic Burden of Periprosthetic Joint Infection in the United States. J. Arthroplasty 2012, 27 (8), 61–65. [PubMed: 22554729]

(6). Zimmerli W; Trampuz A; Ochsner PE, Prosthetic-Joint Infections. N. Engl. J. Med. 2004, 351 (16), 1645–1654. [PubMed: 15483283]

(7). Zmistowski B; Karam JA; Durinka JB; Casper DS; Parvizi J, Periprosthetic Joint Infection Increases the Risk of One-year Mortality. JBJS 2013, 95 (24), 2177–2184.

(8). Campoccia D; Montanaro L; Arciola CR, The Significance of Infection Related to Orthopedic Devices and Issues of Antibiotic Resistance. Biomaterials 2006, 27 (11), 2331–2339. [PubMed: 16364434]

(9). Johnson CT; Wroe JA; Agarwal R; Martin KE; Guldberg RE; Donlan RM; Westblade LF; García AJ, Hydrogel Delivery of Lysostaphin Eliminates Orthopedic Implant Infection by Staphylococcus aureus and Supports Fracture Healing. Proc. Natl. Acad. Sci. USA 2018, 115 (22), E4960–E4969. [PubMed: 29760099]

(10). Southwood R; Rice J; McDonald P; Hakendorf P; Rozenbilds M, Infection in Experimental Hip Arthroplasties. J. Bone Joint. Surg. Br. 1985, 67 (2), 229–231. [PubMed: 3980532]

(11). Donlan RM; Costerton JW, Biofilms: Survival Mechanisms of Clinically Relevant Microorganisms. Clin. Microbiol. Rev. 2002, 15 (2), 167–193. [PubMed: 11932229]

(12). Singh AV; Vyas V; Patil R; Sharma V; Scopelliti PE; Bongiorno G; Podestà A; Lenardi C; Gade WN; Milani P, Quantitative Characterization of the Influence of the Nanoscale Morphology of Nanostructured Surfaces on Bacterial Adhesion and Biofilm Formation. PLoS One 2011, 6 (9), e25029.

(13). Jang Y; Choi WT; Johnson CT; García AJ; Singh PM; Breedveld V; Hess DW; Champion JA, Inhibition of Bacterial Adhesion on Nanotextured Stainless Steel 316l by Electrochemical Etching. ACS Biomater. Sci. Eng. 2018, 4 (1), 90–97. [PubMed: 29333490]

(14). Giavaresi G; Meani E; Sartori M; Ferrari A; Bellini D; Sacchetta AC; Meraner J; Sambri A; Vocale C; Sambri V, Efficacy of Antibacterial-loaded Coating in an in Vivo Model of Acutely Highly Contaminated Implant. Int. Orthop. 2014, 38 (7), 1505–1512. [PubMed: 24363076]

(15). Ashbaugh AG; Jiang X; Zheng J; Tsai AS; Kim WS; Thompson JM; Miller RJ; Shahbazian JH; Wang Y; Dillen CA, Polymeric Nanofiber Coating with Tunable Combinatorial Antibiotic Delivery Prevents Biofilm-associated Infection in Vivo. Proc. Natl. Acad. Sci. USA 2016, 113 (45), E6919–E6928. [PubMed: 27791154]

(16). Li B; Brown KV; Wenke JC; Guelcher SA, Sustained Release of Vancomycin from Polyurethane Scaffolds Inhibits Infection of Bone Wounds in a Rat Femoral Segmental Defect Model. J. Control. Release 2010, 145 (3), 221–230. [PubMed: 20382191]

(17). Hanssen AD; Spangehl MJ, Practical Applications of Antibiotic-loaded Bone Cement for Treatment of Infected Joint Replacements. Clin. Orthop. Relat. Res. 2004, (427), 79–85.

(18). Anderson EM; Noble ML; Garty S; Ma H; Bryers JD; Shen TT; Ratner BD, Sustained Release of Antibiotic from Poly(2-hydroxyethyl Methacrylate) to Prevent Blinding Infections after Cataract Surgery. Biomaterials 2009, 30 (29), 5675–5681. [PubMed: 19631376]

(19). Penner MJ; Masri BA; Duncan CP, Elution Characteristics of Vancomycin and Tobramycin Combined in Acrylic Bone-cement. J. Arthroplasty 1996, 11 (8), 939–944. [PubMed: 8986572]

(20). Jose B; Antoci V; Zeiger AR; Wickstrom E; Hickok NJ, Vancomycin Covalently Bonded to Titanium Beads Kills Staphylococcus aureus. Chem. Biol. 2005, 12 (9), 1041–1048. [PubMed: 16183028]

(21). Antoci V; King SB; Jose B; Parvizi J; Zeiger AR; Wickstrom E; Freeman TA; Composto RJ; Ducheyne P; Shapiro IM, Vancomycin Covalently Bonded to Titanium Alloy Prevents Bacterial Colonization. J. Orth. Res. 2007, 25 (7), 858–866.

(22). Antoci V Jr.; Adams CS; Hickok NJ; Shapiro IM; Parvizi J, Vancomycin Bound to Ti Rods Reduces Periprosthetic Infection - Preliminary Study. Clin. Orthop. Relat. Res. 2007, (461), 88–95.

(23). Lv J; Xiu P; Tan J; Jia ZJ; Cai H; Liu ZJ, Enhanced Angiogenesis and Osteogenesis in Critical Bone Defects by the Controlled Release of BMP-2 and VEGF: Implantation of Electron Beam Melting-fabricated Porous Ti6Al4V Scaffolds Incorporating Growth Factor-doped Fibrin Glue. Biomed. Mater. 2015, 10 (3).

(24). Lv J; Jia ZJ; Li J; Wang YN; Yang J; Xiu P; Zhang K; Cai H; Liu ZJ, Electron Beam Melting Fabrication of Porous Ti6Al4V Scaffolds: Cytocompatibility and Osteogenesis. Adv. Eng. Mater. 2015, 17 (9), 1391–1398.

(25). Gallardo-Moreno AM; Pacha-Olivenza MA; Saldana L; Perez-Giraldo C; Bruque JM; Vilaboa N; Gonzalez-Martin ML, In Vitro Biocompatibility and Bacterial Adhesion of Physico-chemically Modified Ti6Al4V Surface by Means of UV Irradiation. Acta Biomater. 2009, 5 (1), 181–192. [PubMed: 18768375]

(26). Lee TM; Chang E; Yang CY, Attachment and Proliferation of Neonatal Rat Calvarial Osteoblasts on Ti6Al4V: Effect of Surface Chemistries of the Alloy. Biomaterials 2004, 25 (1), 23–32. [PubMed: 14580905]

(27). Grundmann H; Aires-de-Sousa M; Boyce J; Tiemersma E, Emergence and Resurgence of Meticillin-resistant Staphylococcus aureus as a Public-health Threat. Lancet 2006, 368 (9538), 874–885. [PubMed: 16950365]

(28). Walsh C, Molecular Mechanisms That Confer Antibacterial Drug Resistance. Nature 2000, 406 (6797), 775–781. [PubMed: 10963607]

(29). Kahne D; Leimkuhler C; Wei L; Walsh C, Glycopeptide and Lipoglycopeptide Antibiotics. Chem. Rev. 2005, 105 (2), 425–448. [PubMed: 15700951]

(30). Lawson MC; Shoemaker R; Hoth KB; Bowman CN; Anseth KS, Polymerizable Vancomycin Derivatives for Bactericidal Biomaterial Surface Modification: Structure−Function Evaluation. Biomacromolecules 2009, 10 (8), 2221–2234. [PubMed: 19606854]

(31). Lawson MC; Hoth KC; DeForest CA; Bowman CN; Anseth KS, Inhibition of Staphylococcus epidermidis Biofilms Using Polymerizable Vancomycin Derivatives. Clin. Orthop. Relat. Res. 2010, 468 (8), 2081–2091. [PubMed: 20191335]

(32). Lawson MC; Bowman CN; Anseth KS, Vancomycin Derivative Photopolymerized to Titanium Kills S. epidermidis. Clin. Orthop. Relat. Res. 2007, 461, 96–105. [PubMed: 17549033]

(33). Liu P; Song J, Well-Controlled ATRP of 2-(2-(2-azidoethyoxy)ethoxy)ethyl Methacrylate for High-density Click Functionalization of Polymers and Metallic Substrates. J. Polym. Sci., Part A: Polym. Chem. 2016, 54 (9), 1268–1277.

(34). Kutikov AB; Skelly JD; Ayers DC; Song J, Templated Repair of Long Bone Defects in Rats with Bioactive Spiral-wrapped Electrospun Amphiphilic Polymer/hydroxyapatite Scaffolds. ACS Appl. Mater. Interfaces 2015, 7 (8), 4890–4901. [PubMed: 25695310]

(35). Liu P; Domingue E; Ayers DC; Song J, Modification of Ti6Al4V Substrates with Well-defined Zwitterionic Polysulfobetaine Brushes for Improved Surface Mineralization. ACS Appl. Mater. Interfaces 2014, 6 (10), 7141–7152. [PubMed: 24828749]

(36). Francis KP; Joh D; Bellinger-kawahara C; Hawkinson MJ; Purchio TF; Contag PR, Monitoring Bioluminescent Staphylococcus aureus Infections in Living Mice Using a Novel Luxabcdeconstruct. Infect. Immun. 2000, 68 (6), 3594–3600. [PubMed: 10816517]

(37). Arciola CR; Campoccia D; Montanaro L, Implant Infections: Adhesion, Biofilm Formation and Immune Evasion. Nat. Rev. Microbiol. 2018, 16 (7), 397–409. [PubMed: 29720707]

(38). Moormeier DE; Bayles KW, Staphylococcus aureus Biofilm: A Complex Developmental Organism. Mol. Microbiol. 2017, 104 (3), 365–376. [PubMed: 28142193]

(39). Gelber M; Babushkin F; Schattner A, Stubborn Creatures: Dormant Staphylococcus aureus. Am. J. Med. 2017, 130 (3), e101–e102. [PubMed: 28215948]

(40). Funao H; Ishii K; Nagai S; Sasaki A; Hoshikawa T; Aizawa M; Okada Y; Chiba K; Koyasu S; Toyama Y, Establishment of a Real-time, Quantitative, and Reproducible Mouse Model of Staphylococcus Osteomyelitis Using Bioluminescence Imaging. Infect. Immun. 2012, 80 (2), 733–741. [PubMed: 22104103]

(41). Yokogawa N; Ishikawa M; Nishitani K; Beck CA; Tsuchiya H; Mesfin A; Kates SL; Daiss JL; Xie C; Schwarz EM, Immunotherapy Synergizes with Debridement and Antibiotic Therapy in a Murine 1-stage Exchange Model of MRSA Implant-associated Osteomyelitis. J. Orth. Res. 2018, 36 (6), 1590–1598.

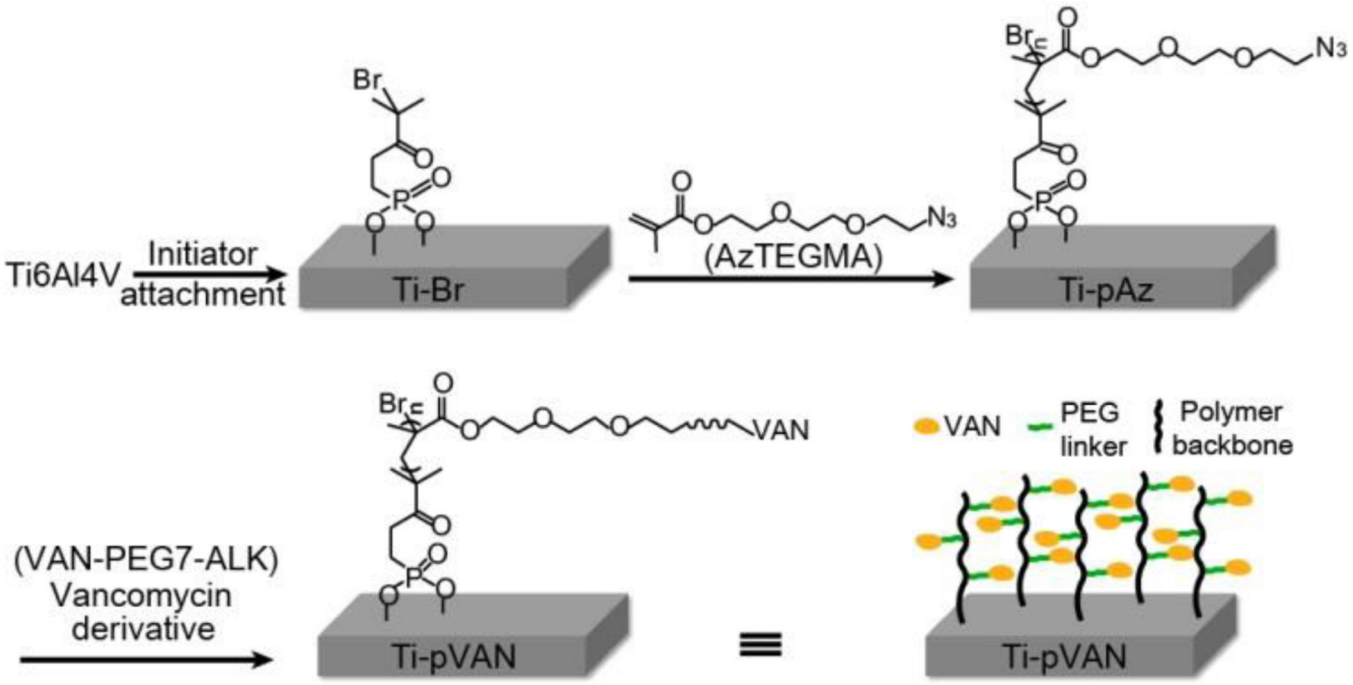

Figure 1.

Synthetic scheme of surface modification of Ti6Al4V by SI-ATRP and CuAAC. Br: bromium, pAzTEGMA: Poly[2-(2-(2-azidoethyoxy)ethoxy)ethyl methacrylate], Az: azide, VAN: vancomycin.

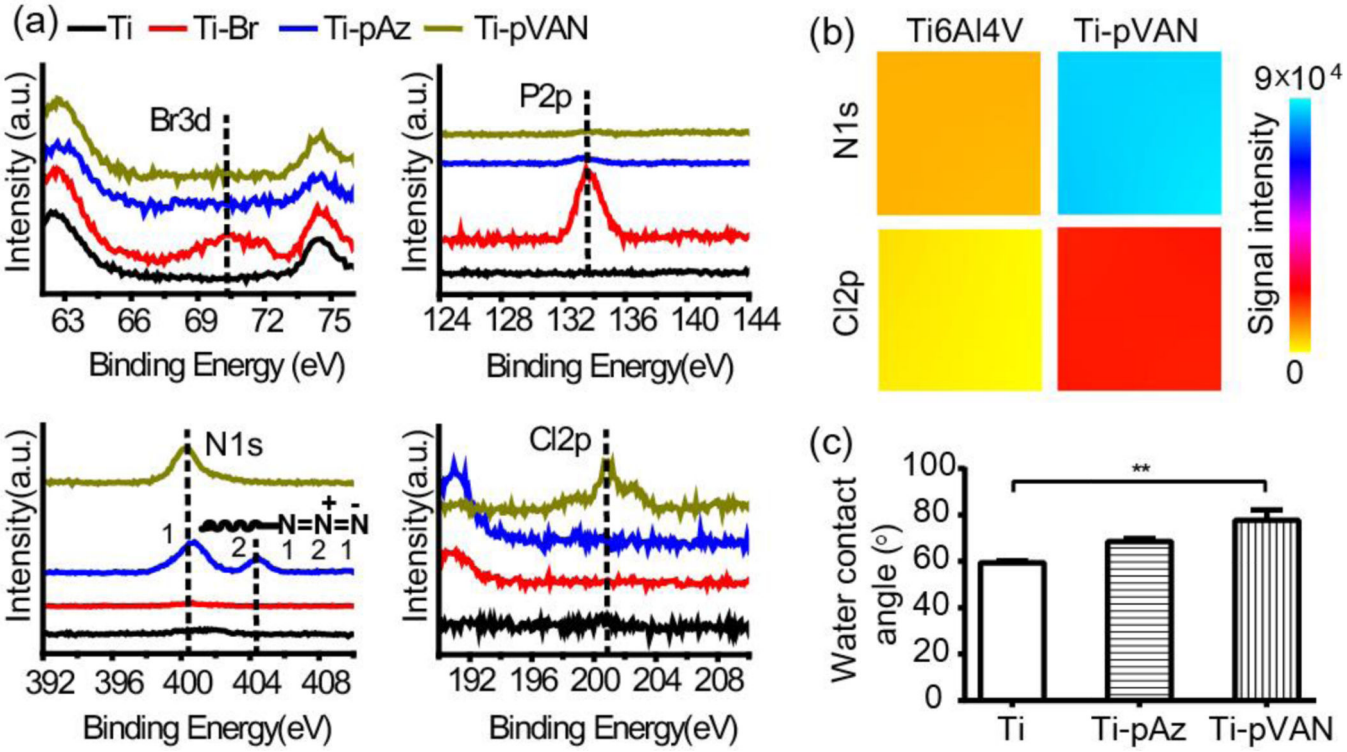

Figure 2.

Surface characterizations of functionalized Ti6Al4V plates. (a) High-resolution scans of XPS spectra. (b) XPS surface elemental color mapping over 400 μm×400 μm areas on unmodified Ti6Al4V and Ti-pVAN plates. (c) Water contact angles (n=3), $^{**}p<0.01$ (One-way ANOVA).

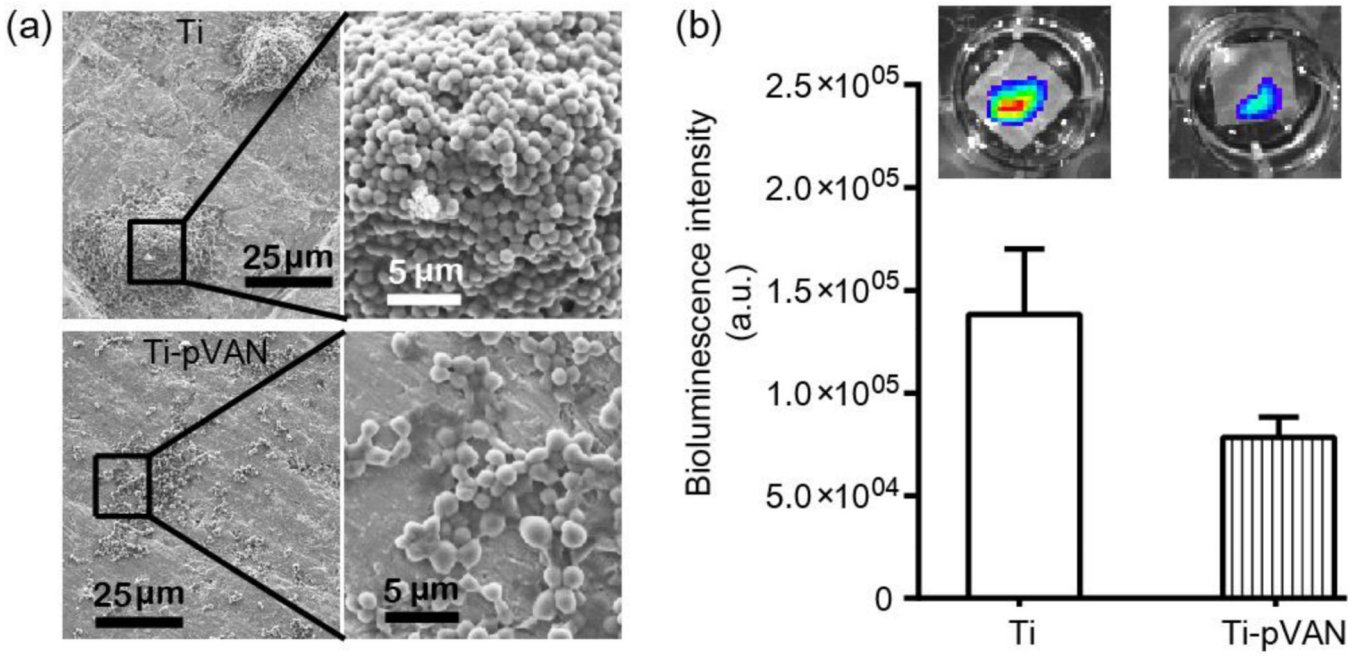

Figure 3.

Ti-pVAN inhibits colonization and growth of *S. aureus in vitro*. (a) SEM of *S. aureus* adhered on unmodified Ti6Al4V and Ti-pVAN plates after 5-h incubation with 1.2×10^5 CFU/mL *S. aureus* in LB at 37 ºC on a shaking incubator (1 Hz). (b) Quantification of bioluminescent signal (n=3) after 7-h incubation of Xen29 *S. aureus* (2.3×10^6 CFU/mL) with unmodified Ti6Al4V vs. Ti-pVAN plates in LB at 37 ºC on a shaking incubator (1 Hz). No significant difference ($p>0.05$, Student's t test). Insets: representative bioluminescent images acquired on IVIS.

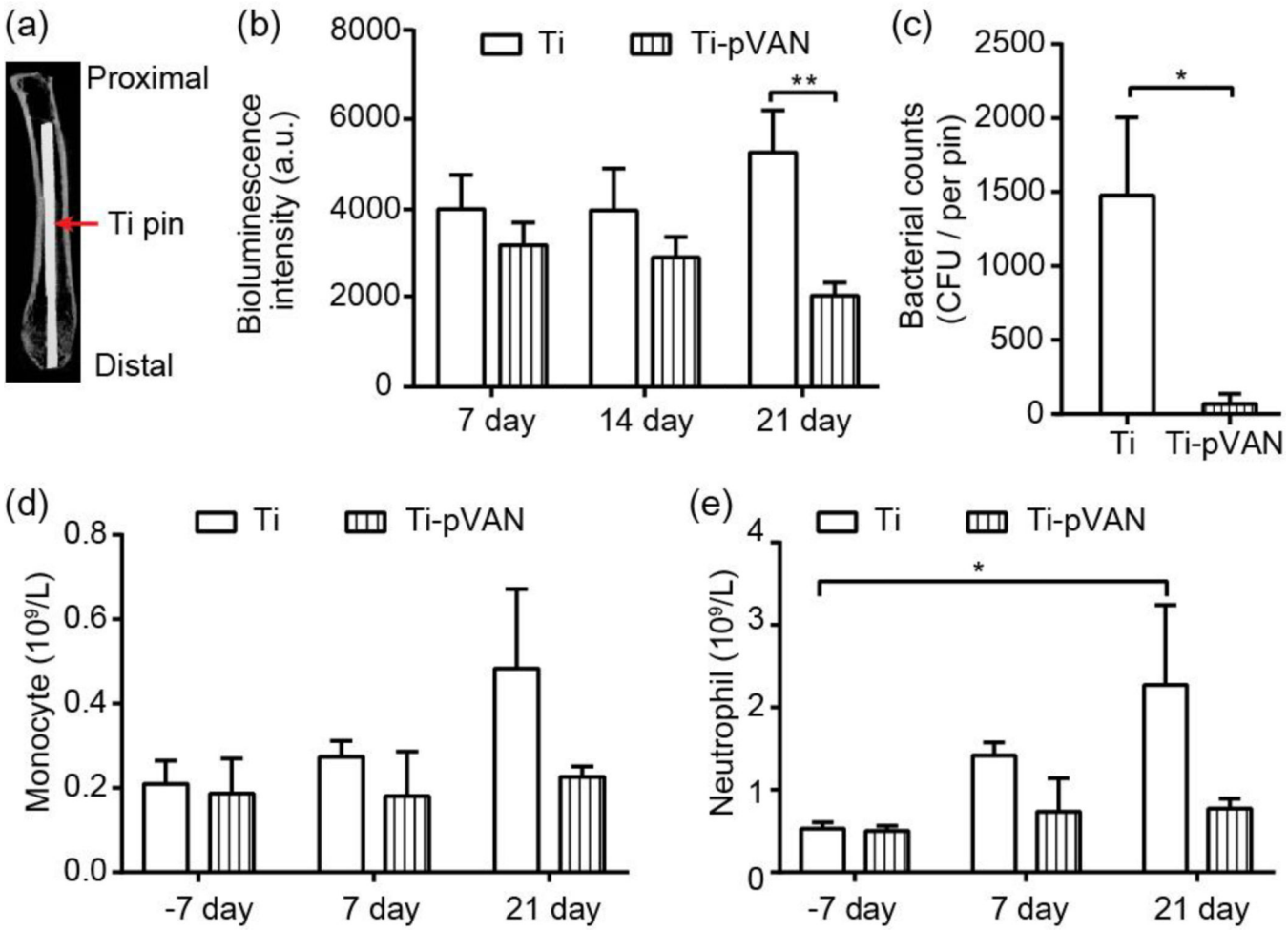

Figure 4.

Ti-pVAN pins suppress *S. aureus* colonization in infected mouse femoral canal and mitigate infection *in vivo*. (a) μ-CT image confirming the proper insertion of an IM Ti6Al4V pin in mouse femoral canal. (b) Longitudinal bioluminescence monitoring of mouse femurs injected with 40 CFU *S. aureus* followed by Ti6Al4V or Ti-pVAN pin insertion (n=8). $^{**}P<0.01$ (Two-way ANOVA). (c) *S. aureus* recovery from 21-day explanted pins (n=7), $^{*}p<0.05$ (Student *t* test). Peripheral blood counts of monocytes (d) and neutrophils (e) before (−7 day) and after surgery (7 and 21 days; n=3). $^{*}p<0.05$ (Two-way ANOVA).

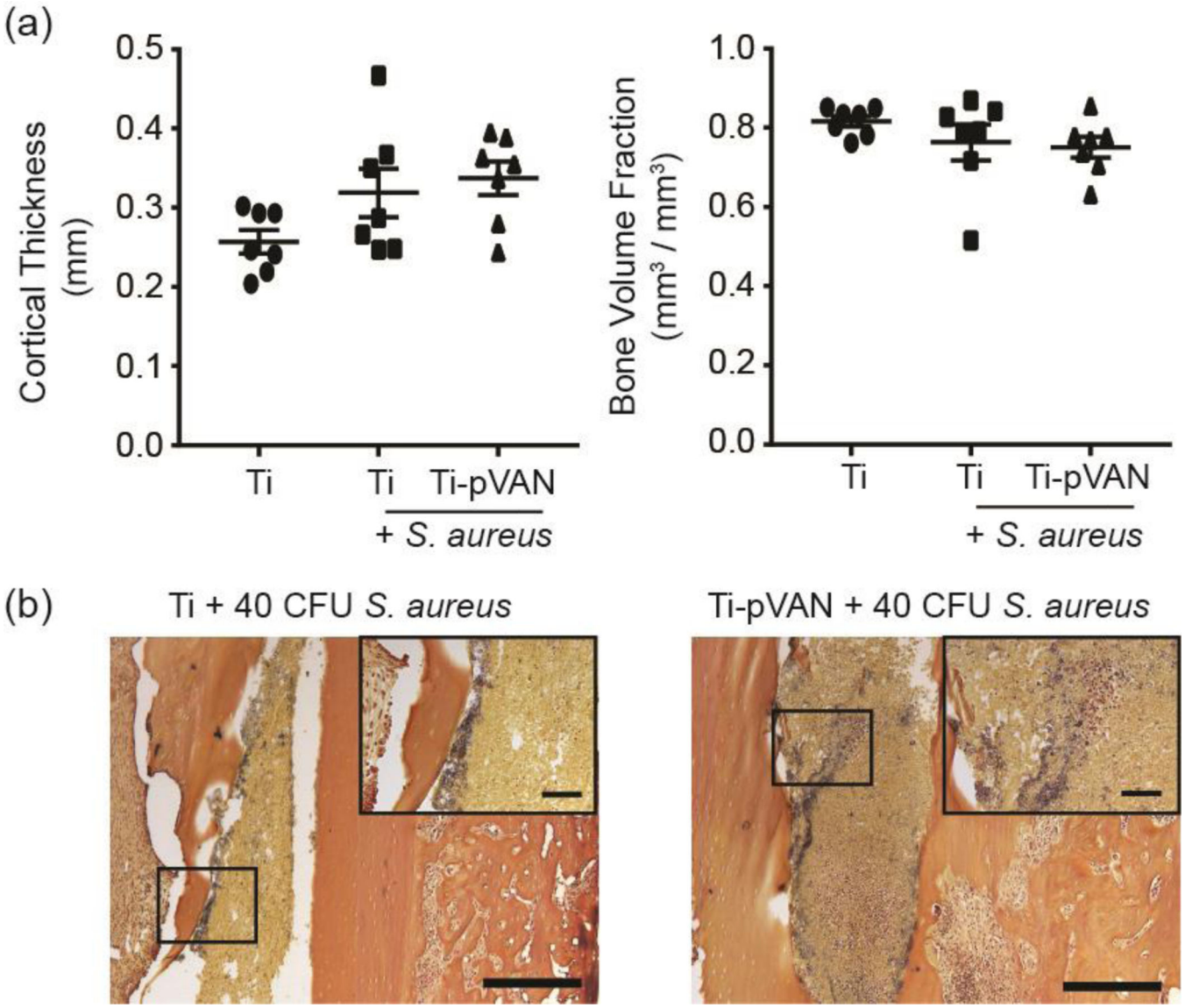

Figure 5.

Ti-pVAN pins do not eradicate *S. aureus* from the endosteal bone surface of infected femoral canal. (a) μ-CT quantification of cortical thickness and bone volume fraction of femur inserted with unmodified Ti6Al4V or Ti-pVAN pins, with or without 40 CFU *S. aureus* (n=7) at 21 days post-op. No significant difference (p>0.05, One-way ANOVA for cortical thickness & Kruskal-Wallis for bone volume fraction). (b) Gram staining of explanted femurs in the infected groups after respective pin removal at 21 days post-op (n=3). Scale bar = 500 μm; Inset: Scale bar = 100 μm.